

The millimeter VLBI Properties of EGRET Blazars

Geoffrey C. Bower
NRAO-Socorro and MPIfR

ABSTRACT

We give a progress report on a snapshot 86 GHz-VLBI survey of the EGRET blazars with the observatories of the CMVA. A high fraction (17/18) of the EGRET blazars were detected on the Pico Veleta-Onsala baseline with a baseline length on the order of 500 $M\lambda$. The detection threshold on the Pico Veleta-Onsala baseline was ~ 0.2 Jy. Six of these sources were not previously detected with 3-millimeter VLBI. We also present the detection of three new non-EGRET sources. The high detection rate for EGRET sources indicates that gamma-ray flux is a robust predictor of millimeter wavelength intensity. Future more sensitive high-energy gamma-ray experiments should find a larger class of objects detectable with millimeter wavelength VLBI.

1. Introduction

A high fraction of high energy gamma-ray sources detected with the EGRET telescope are known to be associated with blazars (Mattox *et al.* 1997). Many of these blazars are among the brightest and most variable sources at millimeter wavelengths. Surveys at centimeter wavelengths have shown that a high fraction of the EGRET blazars are detected on long baselines with VLBI (Moellenbrock *et al.* 1996, Kellerman *et al.* 1998). The conditions necessary to produce high energy gamma-rays are similar to those for compact radio sources.

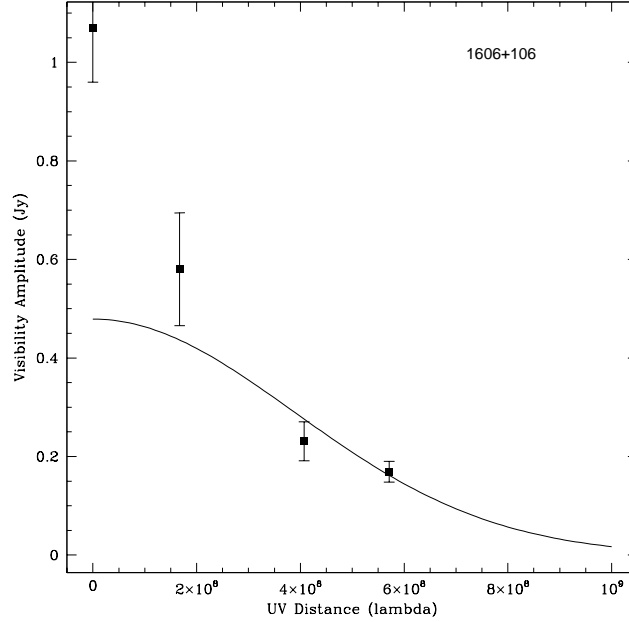
For these reasons, it is likely that many of the EGRET blazars are also millimeter wavelength VLBI sources. Previous source compilations and surveys indicate that the EGRET blazars comprise between 1/3 and 2/3 of all 86 GHz-VLBI detections (Rogers 1994, Lonsdale, Doeleman *et al.* 1998). However, a survey of these objects has not been performed with high sensitivity and under good weather conditions.

We report here on the first epoch of our survey of the EGRET blazars. The full survey will observe all EGRET blazars in the Mattox *et al.* (1997) sample with $\delta > -20^\circ$. All of these sources have $S_5 \gtrsim 1$ Jy and flat spectral indices ($\alpha \gtrsim -0.5$). Additional sources were observed in the program. These were selected from the Moellenbrock *et al.* (1996) and Kellerman *et al.* (1998) surveys as sources with long baseline fluxes greater than ~ 1 Jy.

2. Observations and Results

Observations were made on 2 April 1998 between 0 and 8 UT with a global array of millimeter telescopes. Three sources were observed per hour, each for 6.5 minutes. Additional time was given for pointing and flux density measurements. Due to poor weather and to equipment failures, reliable data was obtained for only 3 stations: Pico Veleta, Bonn and Onsala. Coverage in the visibility plane was essentially linear. Data were correlated at Haystack and analyzed with the Haystack Observatory Post-processing Software (HOPS).

Fig. 1.— Amplitude as a function of baseline length for the EGRET blazar 1606+106. The solid line shows the model Gaussian fit to the three visibility points. The zero-baseline flux is also shown. This source was detected with 3 mm VLBI for the first time in this survey.



Standard polynomial gain curves were applied for Onsala and Bonn. Antenna temperature measurements on source were used to calibrate Pico Veleta. These antenna temperature measurements were also used to determine the zero-baseline flux of the sources.

We summarize in Table 1 the results of detection and model-fitting. Signal-to-noise ratios for the incoherent average are reported. A snr greater than 3.5 is considered a detection. Inspection of the fringe rate and delay solutions for 1739+522 indicates that the detection at $s_{SX} = 3.8$ is firm. Similarly, MK 421 ($s_{SX} = 2.8$) was clearly not detected. The sources 0954+658 and 1219+285 were not observed by Pico Veleta.

Model-fitting was performed in two ways. For sources detected on all three baselines we fit a single Gaussian component to the three visibilities. For sources not detected on the Bonn-Onsala baseline, we fit a single component Gaussian to the zero baseline flux and the Pico Veleta-Onsala visibility. We show in Figure 1 the results for the source 1606+106.

The errors given are the formal error assuming thermal noise and a 10% amplitude calibration error. This significantly underestimates the error for two reasons. First, the source structure may be more complex than a single component. This leads us in most cases to overestimate the size and underestimate the brightness temperature. However, in the event of beating between two components, we may underestimate the size significantly. Second, calibration errors may in fact be much larger than 10%. The low correlated fluxes on the baselines to Bonn for 3C 454.3, BL Lac and CTA 102 are suggestive of a pointing error. These three sources were observed in succession and may have been affected by poor weather.

We do note that for many sources the Gaussian model indicates that most of the zero-baseline flux is

recovered on the short baselines. However, in none of the sources is the zero-baseline flux fully recovered on the long baselines. That is, all sources are resolved to some extent on baseline lengths of $500 M\lambda$.

Closure phases are also included in Table 1. The sources 3C 279 and 3C 454.3 show significantly non-zero closure phases.

3. Discussion

A high fraction (17/18) of the EGRET blazars observed on the Pico Veleta-Onsala baseline were detected. Six of the sources were detected for the first time. The detection threshold on this baselines was ~ 0.2 Jy, making this the most sensitive 3-mm VLBI survey to be performed. Many sources with total fluxes below 1 Jy were detected. We also detected four non-EGRET blazars, three of them for the first time.

The high fraction of EGRET blazars detected supports the conclusion drawn at lower frequencies that peak gamma-ray intensity is a strong predictor of millimeter wavelength intensity. This has several implications.

One, currently unidentified EGRET sources may be associated with specific objects through high frequency VLBI surveys of sources within the error box. The Third EGRET catalog contains 170 unknown sources (Hartman *et al.* 1999). The principal difficulty here will be discriminating the compact non-EGRET blazar sources from the compact EGRET sources.

Two, improvements in gamma-ray telescope sensitivity will produce a much larger class of source available for study. The GLAST mission will be 30 times more sensitive than EGRET, implying a possible increase in the source counts by a factor of ~ 150 . These sources will be of intrinsic interest, of use as a phase and flux calibrators for other areas of research and of use as probes of the intervening molecular gas.

Three, in order for these sources to be accessible to millimeter VLBI, array sensitivity must be improved. The results presented here on the Haystack water vapor radiometer are very encouraging in this regard (Tahmouh & Rogers 1999, these proceedings).

REFERENCES

- Hartman, R.C. *et al.* , 1999, ApJS, 123, 79
Kellermann, K.I., Vermeulen, R.C., Zensus, J.A. & Cohen, M.H., 1998, AJ, 115, 1295
Lonsdale, C., Doeleman, S. & Phillips, R.B., 1998, AJ, 116, 8
Mattox, J.R., *et al.* , 1997, ApJ, 481, 95
Moellenbrock, G.A., et al., 1996, AJ, 111, 2174
Rogers, A.E.E., 1994a, *Workshop on the Coordination of Millimeter VLBI*, Haystack Observatory

Table 1. Blazar Detections at 86 GHz

Source	I ^a (Jy)	s_{BS} ^b	s_{BX} ^c	s_{SX} ^d	S_0 ^e (Jy)	θ ^f (mas)	ϕ ^g (deg)	New?
EGRET sources								
0716+714	1.74	6.8	24.4	26.5	1.27 ± 0.13	0.011 ± 0.075	-7.8 ± 2.9	
0827+243	2.19	3.4	13.6	19.1	1.10 ± 0.12	0.008 ± 0.062	11.4 ± 6.5	
0917+449	0.80	1.9	2.8	9.3	0.80 ± 0.20	0.135 ± 0.010	...	✓
0954+658	0.30	3.2	
MK421	0.20	2.7	3.0	2.8	
1156+295	2.34	10.7	28.3	47.5	0.79 ± 0.08	0.105 ± 0.019	3.5 ± 1.8	
1219+285	0.80	3.3	
1222+216	0.98	1.8	5.6	5.4	0.98 ± 0.22	0.222 ± 0.009	...	✓
3C273B	22.45	76.2	236.0	162.1	16.03 ± 1.61	0.174 ± 0.016	-0.1 ± 1.2	
3C279	22.98	71.6	152.4	145.3	28.09 ± 2.81	0.342 ± 0.016	17.5 ± 0.5	
1406-076	1.30	3.5	13.2	16.6	1.77 ± 0.20	0.291 ± 0.022	53.4 ± 40.1	✓
1502+106	0.77	1.6	2.1	8.5	0.77 ± 0.08	0.217 ± 0.011	...	
1510-089	0.95	3.9	11.2	17.8	1.17 ± 0.13	0.218 ± 0.027	0.8 ± 8.1	
1606+106	1.07	3.4	5.0	6.5	0.48 ± 0.06	0.199 ± 0.016	177.3 ± 56.7	✓
1633+38	2.07	2.8	7.0	34.1	2.07 ± 0.34	0.113 ± 0.011	-21.2 ± 7.4	
1739+522	0.93	2.2	1.7	3.8	0.93 ± 0.27	0.240 ± 0.008	...	✓
BLLAC	4.45	5.6	11.4	74.9	0.72 ± 0.09	0.000 ± 0.039	0.3 ± 5.8	
2209+236	1.02	2.1	2.1	10.5	1.02 ± 0.10	0.193 ± 0.007	...	✓
CTA102	4.84	13.1	29.5	78.1	1.77 ± 0.18	0.002 ± 0.036	-2.3 ± 3.3	
3C454.3	5.62	5.7	26.4	56.1	1.05 ± 0.12	0.001 ± 0.033	22.4 ± 5.3	
non-EGRET sources								
1413+135	2.16	7.9	22.9	32.0	1.29 ± 0.13	0.076 ± 0.031	-1.0 ± 3.5	✓
1655+077	1.53	1.9	7.1	12.1	1.53 ± 0.10	0.244 ± 0.010	...	✓
DA406	2.22	4.4	9.3	16.4	0.45 ± 0.05	0.010 ± 0.069	-5.1 ± 6.3	
NRAO512	0.79	1.8	2.0	5.6	0.79 ± 0.05	0.204 ± 0.008	...	✓

^aZero-baseline flux.

^bIncoherently-averaged SNR for Bonn-Onsala baseline.

^cIncoherently-averaged SNR for Bonn-Pico Veleta baseline.

^dIncoherently-averaged SNR for Pico Veleta-Onsala baseline.

^eTotal flux density of fitted Gaussian component.

^fCircular FWHM of fitted Gaussian component.

^gClosure phase.